

On the Use of Volume Average Constituent Stresses for Predicting Failure in Composites

Kedar A. Malusare¹ and Ray S. Fertig III.²
University of Wyoming, Laramie, WY, 82071

The complexity of the multiple failure mechanisms exhibited by unidirectional fibrous composites makes failure prediction a daunting challenge for the analyst. One approach to better identify failure mechanisms is the use of volume average constituent stresses of the composite and directly predicting constituent failure. However, the total strain energy is not conserved by volume average constituent quantities (stresses and strains). In this study an expression is derived to quantify this missing energy, termed the interaction energy, with the hope of using this energy to enhance the capability of failure prediction using volume average quantities. The variation of interaction energy is studied with respect to the fiber volume fraction, matrix modulus, and biaxial load ratio for typical carbon-epoxy systems. The qualitative relationship between distribution of strain and the interaction energy is analyzed. Finally, the matrix contribution to the interaction energy is examined.

Nomenclature

U	=	total composite strain energy
U_f	=	strain energy contribution of the fiber
U_m	=	strain energy contribution of the matrix
V_c	=	composite volume
V_f	=	total fiber volume
V_f	=	total fiber volume fraction
V_m	=	total matrix volume
V_m	=	total matrix volume fraction
Φ_f	=	fiber interaction energy
Φ_m	=	matrix interaction energy
ε	=	local strain
$\tilde{\varepsilon}$	=	fluctuation in strain
$\langle \varepsilon \rangle$	=	mean strain in the constituent
ε^C	=	composite strain
ε^f	=	strain induced in the fiber
ε^m	=	strain in the matrix constituent
σ^C	=	composite stress
σ^f	=	stress induced in the fiber
σ^m	=	stress in the matrix constituent

¹ Graduate Student, Mechanical Engineering, Dept. 3295, and AIAA Student Member.

² Assistant Professor, Mechanical Engineering, Dept. 3295, Regular Member.

I. Introduction

FIBROUS composites exhibit a range of complex failure behaviors. A variety of theories have been proposed to predict failure in composites [1]. They may be broadly classified into three groups [2], limit or noninteractive theories (maximum stress, maximum strain), interactive theories such as Tsai-Hill and Tsai-Wu [3] and partially interactive theories such as Hashin-Rotem and Puck [4]. Most commonly used failure theories consider individual laminate layers (plies) as building blocks and employ data from simple tests on isolated laminae to predict failure of the entire laminate, a technique called meso-modeling. A well-known composite failure benchmark, the World-Wide Failure Exercise (WWFE), lists five promising theories [5]: Puck [4, 6], Zinoviev [7, 8], Tsai [9, 10], Cuntze [11, 12] and Bogetti [13, 14] for predicting failure in composites which employ the meso-modeling technique. It is well known, that the volume average quantities (stresses and strains) of a lamina do not represent the complex stress/strain state of the constituents, which will be very different than the lamina stresses. But failure of a composite material is always the result of constituent failure, so taking into consideration the stress/strain of the constituents is of vital importance. Micromechanics based theories overcome the drawbacks of meso-modeling by using volume average *constituent* quantities for predicting failure. Micro-modeling involves using experimental data of the properties of the constituents of a composite material to predict the behavior of individual laminae, progressing to the laminate and eventually the entire structure. It is apparent that these theories, when fully developed may have the capability of predicting the response of the entire composite structure even in the absence of lamina test data. Chamis [15, 16], Mayes [17, 18] and Huang [19, 20] are the three micromechanics based failure theories that were judged to be moderate as compared to other theories in the WWFE [5]. Other examples of constituent based failure theories are given elsewhere [21-28].

Regardless of the level of approach (micro or meso) all the theories predict lamina failure relatively well for simple load states, but their deficiencies begin to appear for multi-ply laminates under multiaxial loading, especially with in the presence of non-linearity and large deformations [5]. However, material inhomogeneity introduces stress/strain fluctuations in the constituents of a composite material. Volume average constituent quantities do not acknowledge these fluctuations and as a result, the strain energy computed from the constituent volume average quantities may not account for all the strain energy of the composite. Consequently, any failure theory that depends on volume average constituent stresses must be augmented to incorporate this “missing energy” for improved predictions of composite failure. The focus of this work is to investigate the nature of this “missing energy” and its dependence on fiber volume fraction and material properties under different types of loading conditions.

II. Theoretical Motivation

Consider a general composite material consisting of a fiber and matrix phase. Let U denote the strain energy of this composite under an arbitrary load state. Assuming linear elasticity, this energy can be represented mathematically as

$$U = \frac{1}{2} \int_{V_c} \sigma_{ij}^C \varepsilon_{ij}^C dV_c \quad (1)$$

where σ_{ij}^C and ε_{ij}^C are the composite stresses and the strains, respectively, where repeated ij indicies are summed and integration performed over the entire volume of the composite V_c . Equation (1) can be readily written in terms of average composite properties [29]

$$U = \frac{1}{2} \langle \sigma_{ij}^C \rangle \langle \varepsilon_{ij}^C \rangle V_c \quad (2)$$

where the terms in the brackets denote volume average quantities. Equation (1) may be separated into contributions from the fiber and the matrix as

$$U = U_f + U_m \quad (3)$$

where

$$U_f = \frac{1}{2} \int_{V_f} \sigma_{ij}^f \varepsilon_{ij}^f dV_f \quad (4)$$

$$U_m = \frac{1}{2} \int_{V_m} \sigma_{ij}^m \varepsilon_{ij}^m dV_m \quad (5)$$

where the superscripts f and m denote quantities for fiber and matrix, respectively. In contrast to using composite averaged stresses, when using constituent average stresses and strains, all of the strain energy is not accounted for by summing the volume average contributions. This unaccounted strain energy is termed interaction energy. To quantify this the strain energies in the fiber and matrix are written as

$$U_f = \frac{1}{2} \langle \sigma_{ij}^f \rangle \langle \varepsilon_{ij}^f \rangle V_f + \Phi_f V_f \quad (6)$$

$$U_m = \frac{1}{2} \langle \sigma_{ij}^m \rangle \langle \varepsilon_{ij}^m \rangle V_m + \Phi_m V_m \quad (7)$$

where Φ_f and Φ_m are the interaction energy contribution from each constituent strain energies of the fiber and the matrix, respectively. Adding Eqs. (6) and (7) gives the total strain energy of the composite as

$$U_f + U_m = \frac{1}{2} \langle \sigma_{ij}^f \rangle \langle \varepsilon_{ij}^f \rangle V_f + \frac{1}{2} \langle \sigma_{ij}^m \rangle \langle \varepsilon_{ij}^m \rangle V_m + \Phi_f V_f + \Phi_m V_m \quad (8)$$

$$U_f + U_m = \frac{1}{2} \langle \sigma_{ij}^f \rangle \langle \varepsilon_{ij}^f \rangle V_f + \frac{1}{2} \langle \sigma_{ij}^m \rangle \langle \varepsilon_{ij}^m \rangle V_m + \Delta U \quad (9)$$

where

$$\Delta U = \Phi_f V_f + \Phi_m V_m. \quad (10)$$

The constituent-specific components of the interaction energy can be computed by making use of the fact that inhomogeneities of the material properties give rise to fluctuations in strain $\tilde{\boldsymbol{\varepsilon}}$ thereby giving rise to fluctuations in stress $\tilde{\boldsymbol{\sigma}}$ in the constituents. This may be represented as

$$\tilde{\boldsymbol{\varepsilon}} = \boldsymbol{\varepsilon} - \langle \boldsymbol{\varepsilon} \rangle \quad (11)$$

$$\tilde{\boldsymbol{\sigma}} = \boldsymbol{\sigma} - \langle \boldsymbol{\sigma} \rangle \quad (12)$$

where $\boldsymbol{\varepsilon}$ and $\boldsymbol{\sigma}$ represent the local strain and stress, and $\langle \boldsymbol{\varepsilon} \rangle$ and $\langle \boldsymbol{\sigma} \rangle$ represent the mean strain and stress, respectively. To develop the functional form for the interaction energy, the fiber interaction energy is developed here first. The matrix interaction energy can be derived in a similar manner. Substituting Eqs. (11) and (12) in Eq. (4) gives

$$U_f = \frac{1}{2} \int_{V_f} \left(\langle \sigma_{ij}^f \rangle + \langle \tilde{\sigma}_{ij}^f \rangle \right) \left(\langle \varepsilon_{ij}^f \rangle + \langle \tilde{\varepsilon}_{ij}^f \rangle \right) dV_f. \quad (13)$$

Expanding Eq. (13) yields

$$U_f = \frac{1}{2} \int_{V_f} \langle \sigma_{ij}^f \rangle \langle \varepsilon_{ij}^f \rangle dV_f + \frac{1}{2} \int_{V_f} \tilde{\sigma}_{ij}^f \tilde{\varepsilon}_{ij}^f dV_f + \frac{1}{2} \int_{V_f} \langle \sigma_{ij}^f \rangle \tilde{\varepsilon}_{ij}^f dV_f + \frac{1}{2} \int_{V_f} \tilde{\sigma}_{ij}^f \langle \varepsilon_{ij}^f \rangle dV_f, \quad (14)$$

which on further simplification gives

$$U_f = \frac{1}{2} \langle \sigma_{ij}^f \rangle \langle \varepsilon_{ij}^f \rangle V_f + \frac{1}{2} \int_{V_f} \tilde{\sigma}_{ij}^f \tilde{\varepsilon}_{ij}^f dV_f + \frac{1}{2} \langle \sigma_{ij}^f \rangle \int_{V_f} \tilde{\varepsilon}_{ij}^f dV_f + \frac{1}{2} \langle \varepsilon_{ij}^f \rangle \int_{V_f} \tilde{\sigma}_{ij}^f dV_f \quad (15)$$

since $\tilde{\sigma}_{ij}^f$ and $\tilde{\varepsilon}_{ij}^f$ are local fluctuations, the average fluctuation over the entire volume of the fiber is always zero and so Eq. (15) reduces to

$$U_f = \frac{1}{2} \langle \sigma_{ij}^f \rangle \langle \varepsilon_{ij}^f \rangle V_f + \frac{1}{2} \int_{V_f} \tilde{\sigma}_{ij}^f \tilde{\varepsilon}_{ij}^f dV_f \quad (16)$$

equating Eqs. (6) and (16) gives the expression for interaction energy of the fiber as

$$\Phi_f = \frac{1}{2} \int_{V_f} \tilde{\sigma}_{ij}^f \tilde{\varepsilon}_{ij}^f dV_f \quad (17)$$

Substituting Hooke's law into Eq. (17) allows the interaction energy to be written entirely in terms of strain

$$\Phi_f = \frac{1}{2} \int_{V_f} C_{ijkl} \tilde{\varepsilon}_{ij}^f \tilde{\varepsilon}_{kl}^f dV_f \quad (18)$$

assuming transverse isotropy and expanding Eq. (18) in i, j, k and l yields

$$\Phi_f = \frac{1}{2} \left[C_{11}^f \langle (\tilde{\varepsilon}_{11}^f)^2 \rangle + C_{22}^f \langle (\tilde{\varepsilon}_{22}^f)^2 \rangle + C_{33}^f \langle (\tilde{\varepsilon}_{33}^f)^2 \rangle + 2C_{12}^f \langle \tilde{\varepsilon}_{11}^f \cdot \tilde{\varepsilon}_{22}^f \rangle + 2C_{13}^f \langle \tilde{\varepsilon}_{11}^f \cdot \tilde{\varepsilon}_{33}^f \rangle + \right. \\ \left. 2C_{23}^f \langle \tilde{\varepsilon}_{22}^f \cdot \tilde{\varepsilon}_{33}^f \rangle + C_{12}^f \langle (\tilde{\gamma}_{12}^f)^2 \rangle + C_{13}^f \langle (\tilde{\gamma}_{13}^f)^2 \rangle + C_{23}^f \langle (\tilde{\gamma}_{23}^f)^2 \rangle \right] \quad (19)$$

The interaction energy for the matrix can be similarly shown to be

$$\Phi_m = \frac{1}{2} \left[C_{11}^m \langle (\tilde{\varepsilon}_{11}^m)^2 \rangle + C_{22}^m \langle (\tilde{\varepsilon}_{22}^m)^2 \rangle + C_{33}^m \langle (\tilde{\varepsilon}_{33}^m)^2 \rangle + 2C_{12}^m \langle \tilde{\varepsilon}_{11}^m \cdot \tilde{\varepsilon}_{22}^m \rangle + 2C_{13}^m \langle \tilde{\varepsilon}_{11}^m \cdot \tilde{\varepsilon}_{33}^m \rangle + \right. \\ \left. 2C_{23}^m \langle \tilde{\varepsilon}_{22}^m \cdot \tilde{\varepsilon}_{33}^m \rangle + C_{12}^m \langle (\tilde{\gamma}_{12}^m)^2 \rangle + C_{13}^m \langle (\tilde{\gamma}_{13}^m)^2 \rangle + C_{23}^m \langle (\tilde{\gamma}_{23}^m)^2 \rangle \right] \quad (20)$$

Eqs. (19) and (20) represent the quantification of the interaction energy between fiber and matrix, but combined they contain a total of 18 terms. The focus of the subsequent modeling effort is to determine the significance of the interaction energy relative to the total strain energy, to investigate how the interaction energy may change as a function of loading and material properties, and to attempt to establish whether one constituent is the dominant contributor to interaction energy.

III. Modeling

A. Overview

The goal of the modeling effort is to investigate the variation of interaction energy ΔU with fiber volume fraction and the elastic moduli of the constituents under different loading conditions and to evaluate specific contributions of each constituent. This was accomplished by constructing and exercising a finite element model using the commercially available FEA software ABAQUS. For the purpose of analysis a representative volume element (RVE) having hexagonal fiber packing was considered. The RVE is rectangular and has one fiber section at the center and a quarter section of fiber at each vertex. The rest of the RVE consists of the matrix. This is shown in Fig. 1, where the fiber region is shaded in dark green surrounded by a gray matrix region. The fibers are assumed to be unidirectional along the 1-axis.

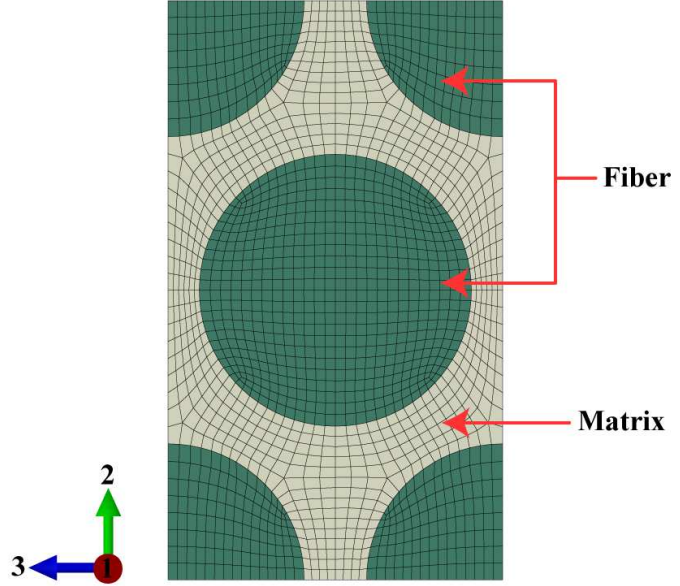


Figure 1: RVE with hexagonal fiber packing for fiber volume fraction of 0.6

B. Material Properties

The fiber material selected for all the simulations was carbon (AS4). The detailed fiber properties are taken from [29] and presented in Table 1. For all the simulations, the fiber properties were kept constant. The matrix was assumed to be isotropic with a Poisson's ratio of 0.34. Three types of variations were studied. First, the fiber volume fraction was varied from 0.05 to 0.85. In the second study, the matrix modulus was varied from 1% to 120% of the fiber modulus (in the fiber direction). A matrix modulus of around $0.0204E_{1fiber}$ ($E_m = 4.8$ GPa) corresponds to epoxy 3501-6. Results were obtained for four different fiber volume fractions of 0.05, 0.25, 0.6 and 0.85. In the third study, four types of biaxial loads were applied, the matrix modulus and fiber volume fraction being constant at $0.01702E_{1fiber}$ ($E_m = 4.0$ GPa) and 0.6 respectively.

C. Boundary Conditions

Periodic boundary conditions were applied on all RVE edges, faces, and corners. This was achieved by extracting nodes from the RVE after meshing, reordering them properly, and using equation constraints for the node sets. For the first two studies, six loads were applied to the RVE in separate steps. These loads were in the form of strains, which were achieved by fixing displacements of the control nodes that render movement to faces in three directions. A strain of 0.01 was applied in each load case, with all other strains held fixed at zero.

Table 1: Baseline material properties of the fiber

Material	Type	E_1 (GPa)	E_2 (GPa)	G_{12} (GPa)	ν_{12}	ν_{23}
AS4	Transversely isotropic	235	14	28	0.2	0.25

In the third study, strains were applied so that they produced a biaxial load of 10MPa. The RVE was subjected to five types of biaxial loads: $\sigma_{22} - \sigma_{33}$, $\sigma_{12} - \sigma_{22}$, $\sigma_{12} - \sigma_{23}$, $\sigma_{12} - \sigma_{13}$ and lastly, $\sigma_{23} - \sigma_{22}$. These loads were applied such that they corresponded to the x- and y-components of the biaxial load represented as the radius of a circle as shown in Fig. 2 and θ is varied from 0° to 180° . The two uniaxial loads required to generate the biaxial load state can be expressed as

$$\sigma_I = \sigma \cos \theta \quad (21)$$

$$\sigma_{II} = \sigma \sin \theta \quad (22)$$

where σ is the resultant bi-axial load and, σ_I and σ_{II} are the corresponding uniaxial loads.

IV. Results and Discussion

As discussed above, three series of simulations were carried out to quantify the dependencies of the interaction energy on material properties, fiber volume fraction, and loading conditions: (i) constant matrix and fiber modulus with varying fiber volume fraction, (ii) varying matrix modulus for four different fiber volume fractions, and (iii) constant material and microstructure properties with varying biaxial loading conditions.

A. Variation of Interaction Energy with Fiber Volume Fraction

For the first series of simulations, the matrix modulus was fixed at 1% of the fiber-direction fiber modulus, $E_m = 2.35GPa$. The fiber volume fraction was varied from 0.05 to 0.85. Volume average quantities (stresses, strains and stiffness) of the composite were extracted from the model and then the total strain energy for the composite was calculated using Eq. (2). The volume average quantities (stresses, strains and stiffness) of the constituents were also extracted. From composite and constituent strains, constituent strain fluctuations were computed using Eq. (11). Substituting these strain fluctuations and the stiffness in Eqs. (19) and (20) gives Φ_f and Φ_m . The total interaction energy was computed using Eq. (10). Interaction energies were computed for all the six load cases individually. The interaction energy fraction ($\Delta U/U$) was calculated for all the fiber volume fractions and each load case. The properties of the RVE were transversely isotropic and were identical in the 2- and 3-direction and in 12- and 13-direction. As a result of this, interaction energy of four (and not all six) load cases are unique.

Figure 3 shows ΔU as a function of fiber volume fraction and load case. Three features of these data are of particular interest. First, the interaction energy is strongly dependent on the load case and it can be very significant. For unidirectional (tension-11) loading, the interaction energy is negligible. In contrast, the interaction energy can be more than 30% of the total strain energy for in-plane shear loading (shear-12). Second, for typical volume fractions, interaction energy increases with

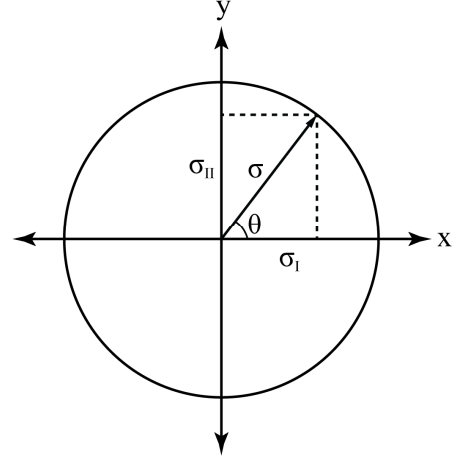


Figure 2: Decomposition of biaxial load into its components

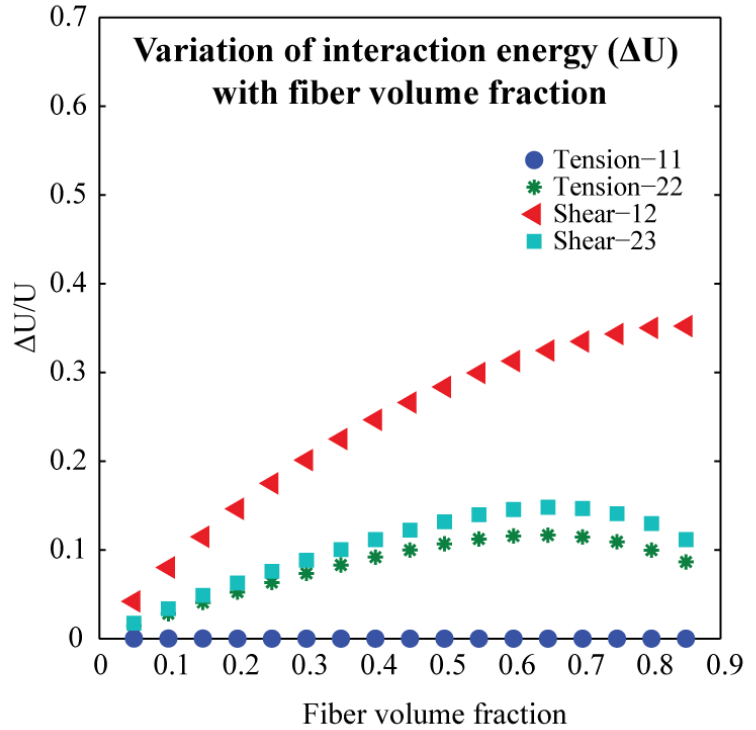


Figure 3: Variation of interaction energy with fiber volume fraction

increasing volume fraction. Finally, transverse tension (tension-22) and transverse shear (shear-23) show a peak at a fiber volume fraction of about 0.65, very close to typical fiber volume fractions in aerospace-grade composites. This behavior can be understood from stress plots of an RVE with a fiber volume fraction of 0.6. In case of tension-11, shown in Fig. 4a, the stress distribution is uniform in each constituent throughout the structure. Thus in this load case strain fluctuations are minimal. Equations. (19) and (20) show that Φ_f and Φ_m are proportional to strain

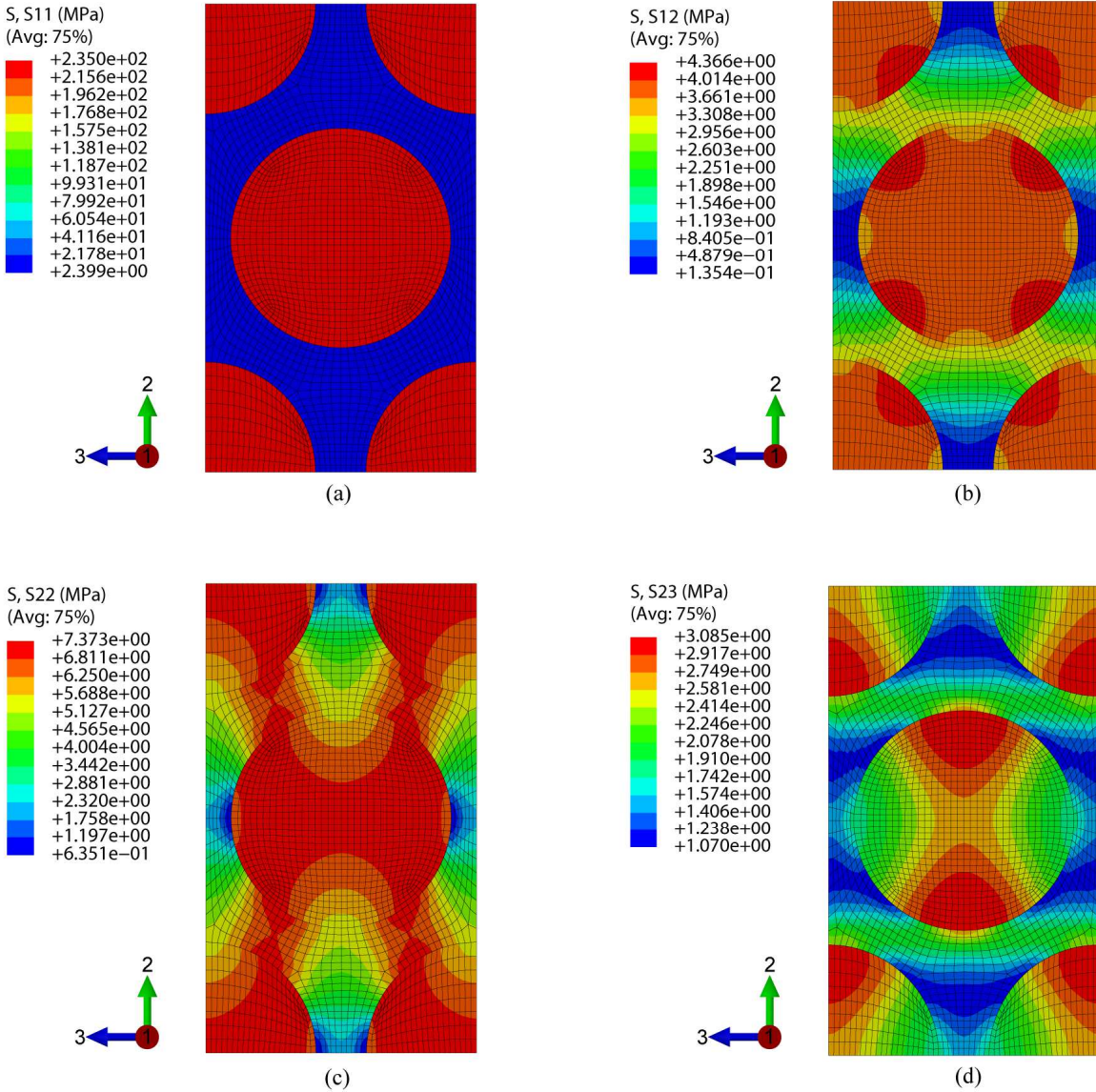


Figure 4: (a) Stress plot for load case tension-11 (b) Stress plot for load case shear-12 (c) Stress plot for load case tension-22 (d) Stress plot for load case shear-23

fluctuation ($\tilde{\epsilon}$), which in turn gives rise to stress fluctuations ($\tilde{\sigma}$) in the constituent. Since there are minimal stress (strain) fluctuations in this load case Φ_f and Φ_m are almost zero for this load case. Consequently the interaction energy ΔU is also zero which is verified by the plot.

In case of shear-12, shown in Fig. 4b, the stress (strain) fluctuation is largest. Consequently the interaction energy is maximum for this case as seen from the plot. This is of vital importance because this peak of interaction energy occurs roughly around the commonly used fiber volume fraction of 0.60. In the load cases tension-22 and shear-23, shown in Fig. 4c and Fig. 4d, respectively, the stress fluctuations are larger than tension-11 and so they have interaction energy higher than tension-11. Figure 5 shows the distribution of strain in load cases shear-12, tension-22 and shear - 23. It can be seen that the distribution of strain in load case shear-23 is smaller than shear-12 but larger than that in load case tension-22, consequently it has an interaction energy less than load case shear-12 but more than tension-22 which is verified by the plot in Fig. 3. It can also be seen that out of the three load cases that have interaction energy, tension-22 has the smallest distribution of strain and so it has the smallest interaction energy.

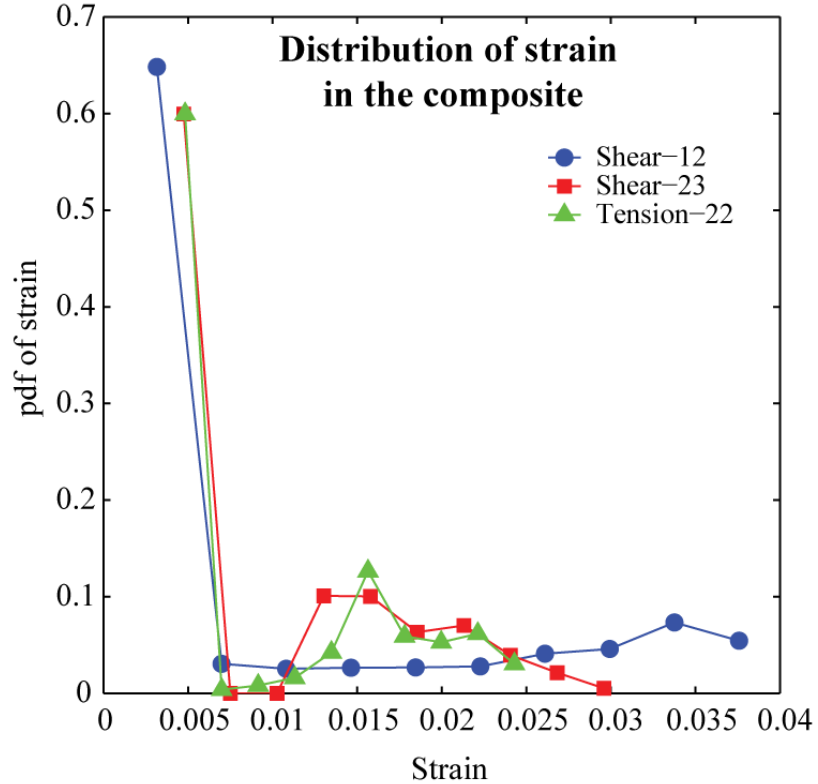


Figure 5 : Probability distribution function for strains for different load cases

B. Variation of interaction energy with matrix modulus

In order to investigate the variation of the interaction energy with matrix modulus, the matrix modulus was varied from 1% to 120% of the fiber-direction fiber modulus. Results were obtained for four fiber volume fractions (0.05, 0.25, 0.60, and 0.85). The interaction energy fraction ($\Delta U/U$) was plotted as a function of the matrix modulus. Figure 6 shows the variation of interaction energy with matrix modulus for the four unique load cases. Fig. 6a shows the variation of interaction energy with matrix modulus in load case tension-11. For this load case, the interaction energy for all volume fractions is negligible. For the other three load cases, shown in Fig. 6b-d, a general trend is observed: an initial increase in matrix modulus results in a decrease in interaction energy until a minimum is reached, after which additional increase in matrix modulus results in an increase in interaction energy. The minimum of the interaction energy occurs when the relevant fiber and matrix stiffnesses are the closest. For the load case in the transverse direction, shown in Fig. 6b, the interaction energy reaches a minimum when the matrix modulus is 5% of the fiber-direction fiber modulus, corresponding to a matrix modulus of 11.75 GPa, which is close to the fiber modulus in the transverse direction of 14 GPa. For a load case of shear-12, shown in Fig. 6c, the interaction energy reaches a minimum when the matrix modulus is 30% of the fiber-direction fiber modulus, corresponding to a matrix shear modulus of 26.31 GPa, which is close to the fiber shear modulus in 12-direction of 28 GPa. For a load case of shear-23, shown in Fig. 6d, the interaction energy reaches a minimum when the matrix

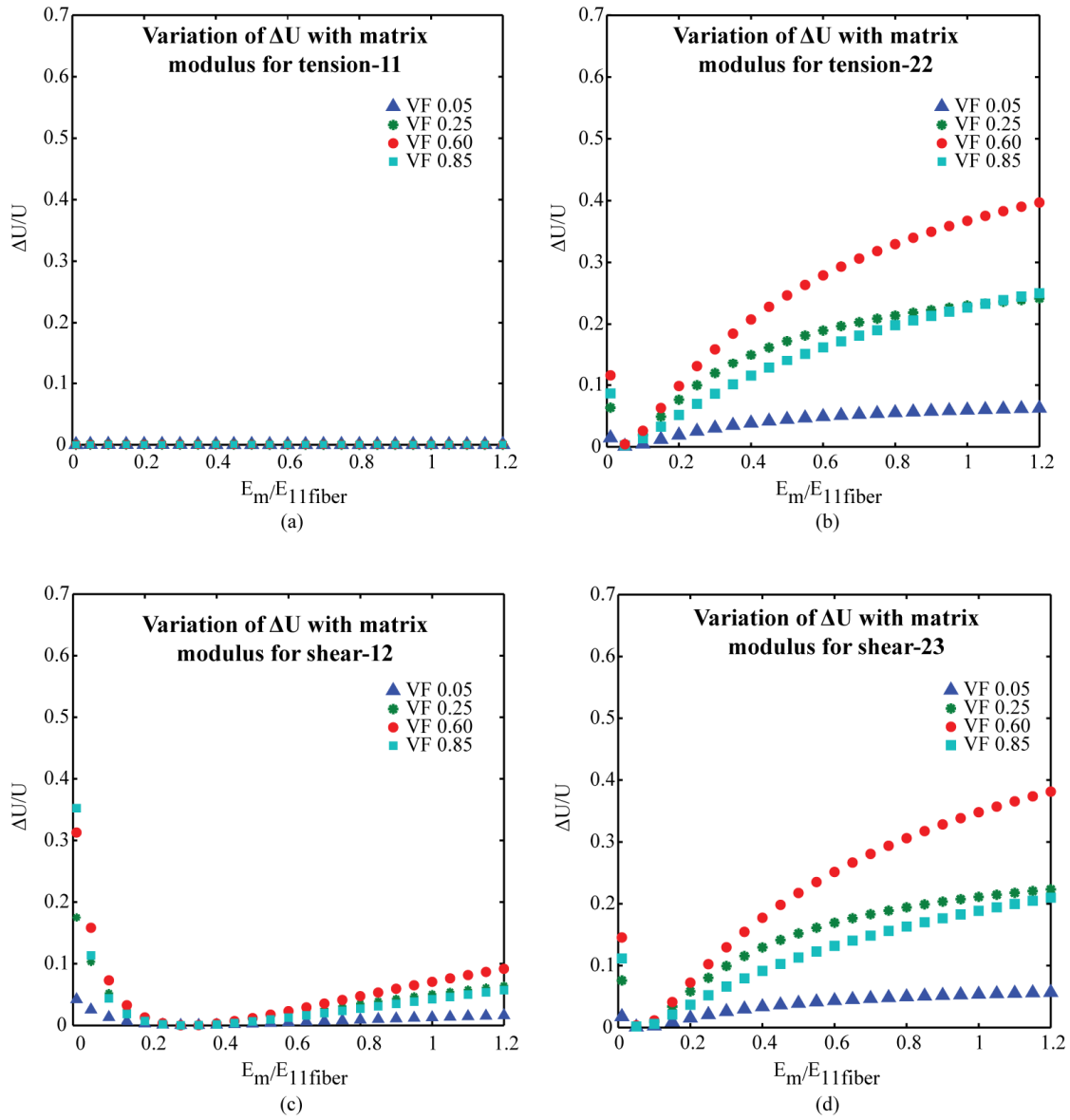


Figure 5: (a) Variation of interaction energy with matrix modulus in load case tension-11 (b) Variation of interaction energy with matrix modulus in load case tension-22 (c) Variation of interaction energy with matrix modulus in load case shear-12 (d) Variation of interaction energy with matrix modulus in load case shear-23

modulus is 5% of the fiber-direction fiber modulus, corresponding to a matrix shear modulus of 4.38 GPa, which is close to the fiber shear modulus in 23-direction of 5.6 GPa. Thus in general, it can be concluded that, for near iso-stress loadings, the interaction energy is proportional to the difference in the fiber and matrix modulus in the loading directions.

C. Variation of interaction energy with biaxial loading

In reality, a composite microstructure is seldom subjected to uniaxial stresses and so it is important to study the behavior of interaction energy under multiaxial load states. Fig. 7 shows the variation of interaction energy under five types of biaxial loadings: $\sigma_{22} - \sigma_{33}$, $\sigma_{12} - \sigma_{22}$, $\sigma_{12} - \sigma_{23}$, $\sigma_{12} - \sigma_{13}$ and lastly, $\sigma_{23} - \sigma_{22}$.

As discussed in Sections A and B, the interaction energy for tensile loading in the 1-direction is negligible. Thus it will not contribute to the interaction energy of the second uniaxial load applied in the fiber direction. The fiber volume fraction and the matrix modulus were kept constant at 0.6 and 4.0 GPa, respectively. The biaxial load is represented by the radius of a circle as shown in Fig 2. θ is the angle made by the radius of the circle with the x-axis which is varied from 0° to 180° so that the effect of biaxial loading on the interaction energy could be quantified. Under a biaxial shear loading in the 12- and 13-directions, it can be observed that the interaction energy does not change but remains constant at 27% of the total strain energy. When the RVE was subjected to a $\sigma_{22} - \sigma_{33}$ biaxial load the interaction energy reached a minimum at 45° . This is because at these two angles, the two stresses are equal to each which results in uniform distribution of strains and stresses in the constituents thereby producing negligible interaction energy shown in Fig. 7.

In the remaining four cases, $\sigma_{12} - \sigma_{23}$, $\sigma_{12} - \sigma_{13}$, $\sigma_{12} - \sigma_{22}$, $\sigma_{23} - \sigma_{22}$ the maximum interaction energy occurs at 90° , which corresponds to a pure shear loading. This result is remarkable: *any* additional applied transverse load reduces the interaction energy that would be computed based on the most significant shear component. The interaction energy can thus be readily bounded by evaluating only a small number of load states.

D. Contribution of Matrix to the Interaction Energy

Interaction energy is a result of material inhomogeneity, which gives rise to strain fluctuations in the constituents. In a two phase composite consisting of fiber and matrix phase, both the fiber and matrix contribute to interaction energy as seen in Eq. (10). The matrix modulus was kept constant at 2.35 GPa and contribution of the matrix to interaction energy was computed. Fig. 8 shows the matrix contribution to interaction energy plotted against fiber volume fraction. The results are remarkable: upto typical fiber volume fractions, the matrix accounts for vast majority of interaction energy. For a commonly used fiber volume fraction of 0.6, the matrix contributes almost entirely (more than 99%) to the interaction energy of the composite for shear loading in the 12-direction. Even for load cases tension-22 and shear-23, matrix contribution to interaction is about 90%. This result is of vital importance since it allows us to altogether neglect the interaction energy of the fiber and focus on modifying the constituent based matrix failure theory.

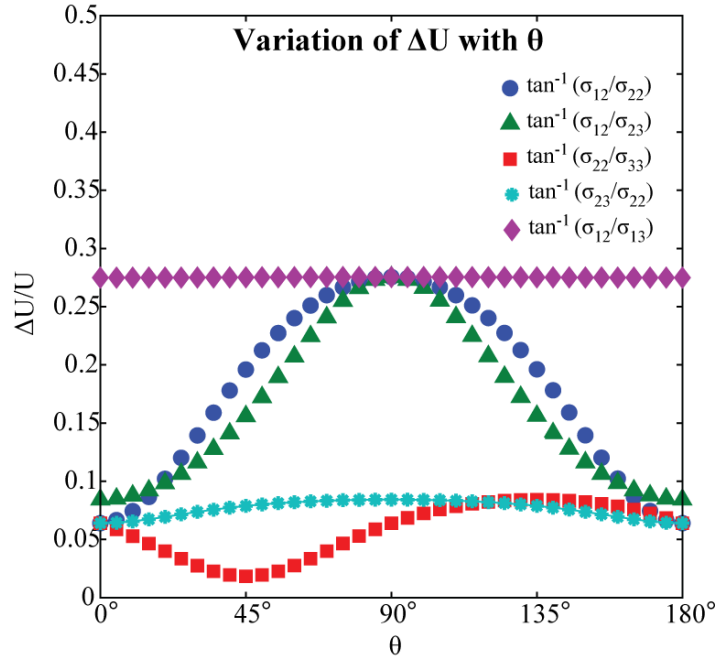


Figure 7 : Variation of interaction energy with biaxial loads.

V. Summary and Conclusions

Fibrous composites are rapidly supplanting conventional homogenous materials like metals in many industries including aerospace, automobile, marine and sports since they are not only lightweight and strong but also chemical and corrosion resistant. Thus precise estimation of composite properties like yield strength, fracture strength, and lifetime has become important. Accurate failure prediction is therefore critical in our efforts towards exploiting the promising advantages offered by composite materials. Although volume average constituent properties (stresses and strains) may not account for all the strain energy of the composite, they are the critical quantities that drive composite failure and are required for genuine physics-based modeling of composites. In this study, an expression was derived to quantify the interaction energy and its dependence on fiber volume fraction and material properties under different

types of loading conditions was examined in hopes of augmenting the use of volume average constituent quantities. Three parametric studies were performed and the interaction energy was computed. It was found that the interaction energy is maximum for composite shear loading in the transverse direction (shear-12) because of maximum strain fluctuations. For typical aerospace-space grade composites, at a common fiber volume fraction of 0.6, the interaction energy is about 30%. Moreover, for such systems, matrix is the major contributor to interaction energy. Interaction energy is directly related to material inhomogeneity and it is always minimum when the relevant fiber and matrix stiffnesses are closest. Interaction energy remains constant under biaxial shear loading. For transverse biaxial loading, interaction energy is minimum when both the transverse loads are equal and is maximum for tension-compression loading.

Failure in composite materials is ultimately a result of constituent failure. Consequently, micromechanics-based failure theories often utilize volume average constituent quantities to apply failure criteria to constituents directly. For accurate failure predictions, any failure theory that employs volume average constituent quantities for failure prediction must incorporate interaction energy. This study has shown that regardless of fiber volume fraction, matrix modulus, or loading conditions, the matrix is the dominant contributor to interaction energy. This result is remarkable because efforts may be channeled towards matrix failure augmentation for superior failure prediction. This study not only elucidates the causes and nature of interaction energy but it also takes us one step closer to realizing the goal of designing with composite materials with the confidence used in designing with more traditional materials.

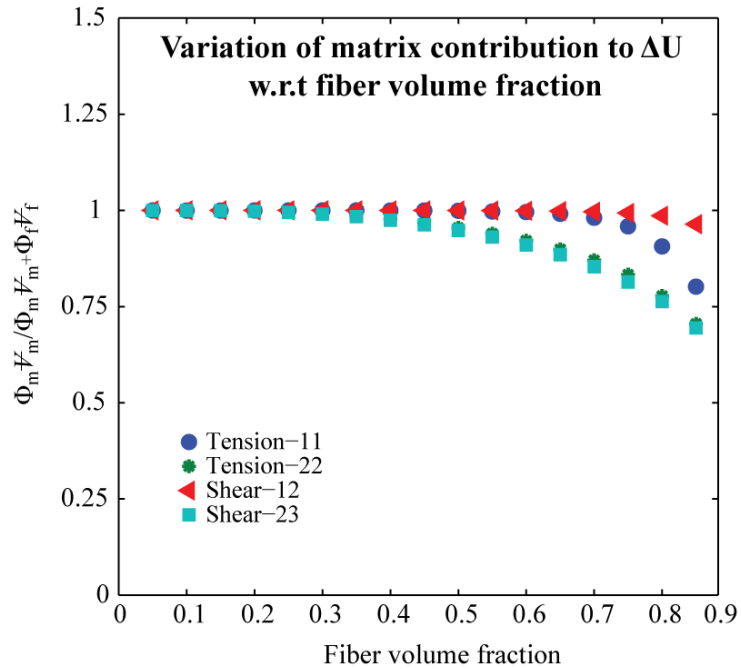


Figure 8: Variation of contribution of matrix to interaction energy with fiber volume fraction

References

1. Echaabi, J., Trochu, F., and Gauvin, R. "Review of failure criteria of fibrous composite materials," *POLYMER COMPOSITES* Vol. 17, No. 6, 1996, pp. 786-798.
doi: 10.1002/pc.10671
2. Daniel, I. M. "Failure of Composite Materials," *Strain* Vol. 43, No. 1, 2007, pp. 4-12.
doi: 10.1111/j.1475-1305.2007.00302.x

3. Tsai, S. W., and Wu, E. M. "A General Theory of Strength for Anisotropic Materials," *Journal of Composite Materials* Vol. 5, No. 1, 1971, pp. 58-80.
4. Puck, A., and Schürmann, H. "Failure analysis of FRP laminates by means of physically based phenomenological models," *Composites Science and Technology* Vol. 62, No. 12–13, 2002, pp. 1633-1662.
doi: [http://dx.doi.org/10.1016/S0266-3538\(01\)00208-1](http://dx.doi.org/10.1016/S0266-3538(01)00208-1)
5. Soden, P. D., Kaddour, A. S., and Hinton, M. J. "Recommendations for designers and researchers resulting from the world-wide failure exercise," *Composites Science and Technology* Vol. 64, No. 3–4, 2004, pp. 589-604.
doi: [http://dx.doi.org/10.1016/S0266-3538\(03\)00228-8](http://dx.doi.org/10.1016/S0266-3538(03)00228-8)
6. Puck, A., and Schürmann, H. "FAILURE ANALYSIS OF FRP LAMINATES BY MEANS OF PHYSICALLY BASED PHENOMENOLOGICAL MODELS," *Composites Science and Technology* Vol. 58, No. 7, 1998, pp. 1045-1067.
doi: [http://dx.doi.org/10.1016/S0266-3538\(96\)00140-6](http://dx.doi.org/10.1016/S0266-3538(96)00140-6)
7. Zinoviev, P. A., Grigoriev, S. V., Lebedeva, O. V., and Tairova, L. P. "The strength of multilayered composites under a plane-stress state," *Composites Science and Technology* Vol. 58, No. 7, 1998, pp. 1209-1223.
doi: [http://dx.doi.org/10.1016/S0266-3538\(97\)00191-7](http://dx.doi.org/10.1016/S0266-3538(97)00191-7)
8. Zinoviev, P. A., Lebedeva, O. V., and Tairova, L. P. "A coupled analysis of experimental and theoretical results on the deformation and failure of composite laminates under a state of plane stress," *Composites Science and Technology* Vol. 62, No. 12–13, 2002, pp. 1711-1723.
doi: [http://dx.doi.org/10.1016/S0266-3538\(01\)00207-X](http://dx.doi.org/10.1016/S0266-3538(01)00207-X)
9. Kuraishi, A., Tsai, S. W., and Liu, K. K. S. "A progressive quadratic failure criterion, part B," *Composites Science and Technology* Vol. 62, No. 12–13, 2002, pp. 1683-1695.
doi: [http://dx.doi.org/10.1016/S0266-3538\(01\)00205-6](http://dx.doi.org/10.1016/S0266-3538(01)00205-6)
10. Liu, K.-S., and Tsai, S. W. "A PROGRESSIVE QUADRATIC FAILURE CRITERION FOR A LAMINATE," *Composites Science and Technology* Vol. 58, No. 7, 1998, pp. 1023-1032.
doi: [http://dx.doi.org/10.1016/S0266-3538\(96\)00141-8](http://dx.doi.org/10.1016/S0266-3538(96)00141-8)
11. Cuntze, R. G., and Freund, A. "The predictive capability of failure mode concept-based strength criteria for multidirectional laminates," *Composites Science and Technology* Vol. 64, No. 3–4, 2004, pp. 343-377.
doi: [http://dx.doi.org/10.1016/S0266-3538\(03\)00218-5](http://dx.doi.org/10.1016/S0266-3538(03)00218-5)
12. Cuntze, R. G. "The predictive capability of failure mode concept-based strength criteria for multi-directional laminates—part B," *Composites Science and Technology* Vol. 64, No. 3–4, 2004, pp. 487-516.
doi: [http://dx.doi.org/10.1016/S0266-3538\(03\)00225-2](http://dx.doi.org/10.1016/S0266-3538(03)00225-2)
13. Bogetti, T. A., Hoppel, C. P. R., Harik, V. M., Newill, J. F., and Burns, B. P. "Predicting the nonlinear response and failure of composite laminates: correlation with experimental results," *Composites Science and Technology* Vol. 64, No. 3–4, 2004, pp. 477-485.
doi: [http://dx.doi.org/10.1016/S0266-3538\(03\)00223-9](http://dx.doi.org/10.1016/S0266-3538(03)00223-9)
14. Bogetti, T. A., Hoppel, C. P. R., Harik, V. M., Newill, J. F., and Burns, B. P. "Predicting the nonlinear response and progressive failure of composite laminates," *Composites Science and Technology* Vol. 64, No. 3–4, 2004, pp. 329-342.
doi: [http://dx.doi.org/10.1016/S0266-3538\(03\)00217-3](http://dx.doi.org/10.1016/S0266-3538(03)00217-3)
15. Gotsis, P. K., Chamis, C. C., and Minnetyan, L. "Application of progressive fracture analysis for predicting failure envelopes and stress–strain behaviors of composite laminates: a comparison with experimental results," *Composites Science and Technology* Vol. 62, No. 12–13, 2002, pp. 1545-1559.
doi: [http://dx.doi.org/10.1016/S0266-3538\(02\)00095-7](http://dx.doi.org/10.1016/S0266-3538(02)00095-7)
16. Gotsis, P. K., Chamis, C. C., and Minnetyan, L. "Prediction of composite laminate fracture: micromechanics and progressive fracture," *Composites Science and Technology* Vol. 58, No. 7, 1998, pp. 1137-1149.
doi: [http://dx.doi.org/10.1016/S0266-3538\(97\)00014-6](http://dx.doi.org/10.1016/S0266-3538(97)00014-6)
17. Mayes, J. S., and Hansen, A. C. "A comparison of multicontinuum theory based failure simulation with experimental results," *Composites Science and Technology* Vol. 64, No. 3–4, 2004, pp. 517-527.
doi: [http://dx.doi.org/10.1016/S0266-3538\(03\)00221-5](http://dx.doi.org/10.1016/S0266-3538(03)00221-5)
18. Mayes, J. S., and Hansen, A. C. "Composite laminate failure analysis using multicontinuum theory," *Composites Science and Technology* Vol. 64, No. 3–4, 2004, pp. 379-394.
doi: [http://dx.doi.org/10.1016/S0266-3538\(03\)00219-7](http://dx.doi.org/10.1016/S0266-3538(03)00219-7)
19. Huang, Z.-M. "A bridging model prediction of the ultimate strength of composite laminates subjected to biaxial loads," *Composites Science and Technology* Vol. 64, No. 3–4, 2004, pp. 395-448.

doi: [http://dx.doi.org/10.1016/S0266-3538\(03\)00220-3](http://dx.doi.org/10.1016/S0266-3538(03)00220-3)

20. Huang, Z.-M. "Correlation of the bridging model predictions of the biaxial failure strengths of fibrous laminates with experiments," *Composites Science and Technology* Vol. 64, No. 3-4, 2004, pp. 529-548.

doi: [http://dx.doi.org/10.1016/S0266-3538\(03\)00222-7](http://dx.doi.org/10.1016/S0266-3538(03)00222-7)

21. Welsh, J. S., Mayes, J. S., and Biskner, A. C. "2-D biaxial testing and failure predictions of IM7/977-2 carbon/epoxy quasi-isotropic laminates," *Composite Structures* Vol. 75, No. 1-4, 2006, pp. 60-66.

doi: DOI: 10.1016/j.compstruct.2006.04.049

22. Fertig III, R. S. "A computationally efficient method for multiscale modeling of composite materials: Extending multicontinuum theory to complex 3D composites," *SAMPE 2010 Fall Technical Conference*. SAMPE, Salt Lake City, UT, 2010, pp. 11-11.

23. Fertig III, R. S. "Bridging the gap between physics and large-scale structural analysis: a novel method for fatigue life prediction of composites," *SAMPE 2009 Fall Technical Conference*. Wichita, KS, 2009.

24. Fertig III, R. S. "An accurate and efficient method for constituent-based progressive failure modeling of a woven composite," *TMS 2010 Annual Meeting*. Vol. 2, TMS, Seattle, WA, 2010, pp. 223-230.

25. Fertig III, R. S., and Kenik, D. J. "Predicting Composite Fatigue Life Using Constituent-Level Physics," *52nd AIAA/ASME/ASCE/AHS/ASC Structures, Structural Dynamics and Materials Conference*. AIAA, Denver, CO, 2011, pp. 11-11.

26. Fertig III, R. S., and Kenik, D. J. "Physics-Based Fatigue Life Prediction of Composite Structures," *NAFEMS World Congress 2011*. Vol. CD-ROM, NAFEMS, Boston, MA, 2011, p. 12.

27. Fertig III, R. S., Stack, J., and Biskner, A. "Modeling Damage Tolerance in Composite Structures: Selecting Material Parameters," *SAMPE 2011*. SAMPE, Long Beach, CA, 2011, p. 13.

28. Reifsnider, K. L., and Gao, Z. "A micromechanics model for composites under fatigue loading," *International Journal of Fatigue* Vol. 13, No. 2, 1991, pp. 149-156.

doi: Doi: 10.1016/0142-1123(91)90007-1

29. Sun, C. T., and Vaidya, R. S. "Prediction of composite properties from a representative volume element," *Composites Science and Technology* Vol. 56, No. 2, 1996, pp. 171-179.

doi: 10.1016/0266-3538(95)00141-7